Supporting information

Substituent Tailoring Anti-Aromaticity and Charge Transport Polarity of Cyclopenta[hi]aceanthrylenes

Wenjing Chen,[ab] Fan Sun,[acd] Junfeng Guo,[ae] Fengxiang Qie,[c] Xiaohui Jia*[b], Chunfeng Shi*[c] and Yonggang Zhen*[a]

Materials and methods

Unless otherwise noted, all chemicals were purchased from commercial suppliers and used without further purification unless otherwise specified. Nitrogen atmosphere is chosen, if there are not special notice. Br-CPAA and TMA-CPAA were prepared according to the known procedure.[1]

Mass spectra (MALDI-TOF-MS) were determined on a Bruker BIFLEX III Mass Spectrometer, and High resolution mass spectra (HRMS) were determined on IonSpec 4.7 Tesla Fourier Transform Mass Spectrometer.

Nuclear Magnetic Resonance (NMR) spectra were recorded on 400 MHz Bruker AVANCE III spectrometers, using chloroform-d ($CDCl_3$) as solvent. Chemical shifts were reported in ppm. Coupling constants (J values) were reported in Hertz.

We carried out nucleus-independent chemical shifts (NICS) calculations and anisotropy of the induced current density (AICD) using the B3LYP functional[2] and 6-311G(d,p) basis set implemented in Gaussian 16 program.[3] Centroid and magnetic shielding tensor were all calculated in Multiwfn 3.8.[4] Density functional theory (DFT) calculations for highest occupied molecular orbital (HOMO) and lowest unoccupied molecular orbital (LUMO) levels were performed at B3LYP/6-311G(d,p) level. The transfer integrals were calculated by the direct method with site-energy correction.[5]

Absorption spectra were measured with SHIMADZU UV-2660i UV-vis spectrophotometer in 1×10^{-5} M solution of TMS-CPAA and CN-CPAA in chloroform with 1-cm quartz cell. Absorption spectra of spin-coated thin film of TMS-CPAA and CN-CPAA on quartz were also measured by the same UV-vis spectrophotometer. The absorption spectrum of powders of TMS-CPAA and CN-CPAA were performed on

Lambda 1050+ spectrometer using an integrating sphere.

Emission spectra was measured with SHIMADZU RF-6000 spectro fluorophotometer in 8×10^{-6} M solution of TMS-CPAA and CN-CPAA in chloroform with 1-cm quartz cell. The excitation wavelength was set at 245 nm, scanning from 270 nm to 850 nm with increments by 1 nm for TMS-CPAA and CN-CPAA.

Cyclic voltammograms (CV) was run on a CHI660C electrochemistry station in 0.1 M solution of Bu_4NPF_6 in dichloromethane with a scan rate of 100 mV/s (in V vs Fc/Fc^+), using a three-electrode configuration (glassy carbon as working electrode, Pt as counter electrode, and Ag/AgCl as pseudo-reference).

The crystal of TMS-CPAA for carrier transport measurements were grown by the physical vapor transport (PVT) method using a temperature-controlled quartz tube. Ultrapure argon was used as the carrier and protection gas to prevent the compounds from oxidation at high temperatures. OTS-modified SiO_2/Si substrates were put in the crystal growth region where the sublimated molecules from the source region can slowly aggregate and recrystallize on the substrate surface at the cooling zone. The crystal of CN-CPAA for carrier transport measurements were grown by the microspacing in-air sublimation (MAS).

The powder and crystals X-ray diffraction patterns were recorded by Empyrean (PANalytical) with a CuKα source (λ = 1.541 Å). The crystal structures were collected using an X-ray diffractometer (XRD, X-Pert, PANalytic, Netherlands) with Cu radiation (40 KV, 30 mA). Deposition Numbers 2379550 and 2379551 contain the supplementary crystallographic data for this paper. These data are provided free of charge by the joint Cambridge Crystallographic Data Centre and Fachinformationszentrum Karlsruhe Access Structures service.

Optical microscopy was performed on an Olympus BX53M microscope.

SiO_2/Si substrates (300 nm thick SiO_2, C_i = 10 nF/cm^2) were successively cleaned with ultra-pure water (ultrasonic cleaning, power 40%, 10 min), piranha solution (H_2SO_4:H_2O_2 = 7:3, heating in water bath, 15min), deionized water (ultrasonic

cleaning, power 40%, 10 min) and isopropanol (ultrasonic cleaning, power 40%, 10 min). After that, OTS was used to modify the SiO_2/Si substrates to reduce the electron traps. Micro-crystals of TMS-CPAA were deposited on the OTS-modified substrates by the physical vapor transport (PVT) method and micro-crystals of CN-CPAA were deposited on the OTS-modified substrates by the microspacing in-air sublimation (MAS). Consequently, top S/D electrodes were deposited onto the crystals of TMS-CPAA and CN-CPAA at a rate of 0.1 Å s^{-1} under vacuum (<1.0×10^{-6} Pa) with organic nanowires[6] or copper grid (L = 25 μm, W = 290 μm) as shadows masks. The thickness of the electrodes is 40 nm.

OFET fabrication and Characterization: The electrical characterization was performed using a semiconductor parameter analyzer (Keithley 4200 SCS). The width and length of the channel were measured using an optical microscope (Olympus BX53M). The field-effect mobility was calculated from the saturation region with the following equation:

$$\mu = \frac{2L}{WC_i} \left(\frac{\partial \sqrt{I_{SD}}}{\partial V_G} \right)^2$$

Where C_i is the dielectric capacitance per unit area, and W and L are the width and length of the crystal between the electrodes, respectively. The field-effect mobility and the threshold voltage can be extracted by plotting the square root of the saturation current versus the gate voltage and performing linear fitting.[7, 8]

1. Synthesis for CN-CPAA

CN-CPAA

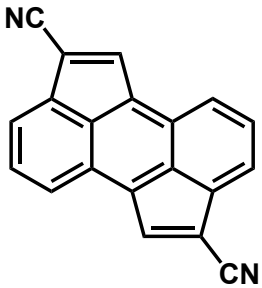

Curpous cyanide (11 g，122.05 mmol) was heated to 160 °C in 70 mL of N methyl-2-pyrrolidone with stirring, Br-CPAA (9.5 g, 24.5 mmol, 1eq) was then added.

The mixture was then stirring at 160 °C for 10 hours. After cooling back to the room temperature, the reaction solution was sedimented in anhydrous ethanol. Removed the solvents, the crude materials were further purified by Soxhlet extraction using chloroform as solvent to remove insoluble impurities. The chloroform solution was collected and subjected to a second sedimentation in anhydrous ethanol. Finally, it was collected by filtration to obtain a black granular solid. Yield: 0.95 g (14%). ^{1}H NMR (400 MHz, Chloroform-*d*) δ 8.33 (d, *J* = 8.4 Hz, 2H), 8.18 (s, 2H), 8.12 (d, *J* = 6.7 Hz, 2H), 7.91 – 7.85 (m, 2H); MS (MALDI-TOF): cacld for M^-, 276.0701; found, 276.0684.

2. The optical characteristics and electrochemical properties of TMS-CPAA and CN-CPAA

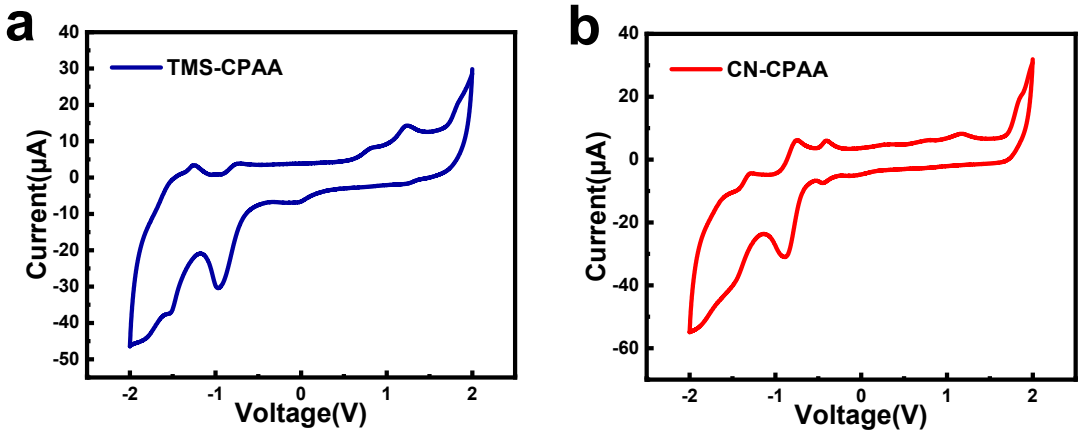

Figure S1. Cyclic voltammograms of compound **TMS-CPAA** (a) and **CN-CPAA** (b).

Table S1 The optical characteristics and electrochemical properties of **TMS-CPAA** and **CN-CPAA**

Compounds	E_{1r}[a](V)	E_{1o}[b](V)	E_g[c](eV)	LUMO (eV)	HOMO (eV)
TMS-CPAA	-	0.31	2.62	–2.49[e]	–5.11[d]
CN-CPAA	–1.21	-	2.50	–3.59[d]	–6.09[e]

a) Half-wave reduction potentials vs. Fc/Fc^+;

b) Half-wave oxidation potentials vs. Fc/Fc^+;

c) E_g values were estimated from the solution absorption spectra;

d) LUMO/HOMO levels were estimated by using the following equation: LUMO level = $-(E_{1r}+4.80)$, HOMO level = $-(E_{1o}+4.80)$;

e) LUMO/HOMO levels were estimated by combination of HOMO/LUMO levels and the *E*g values.

3. XRD for TMS-CPAA and CN-CPAA

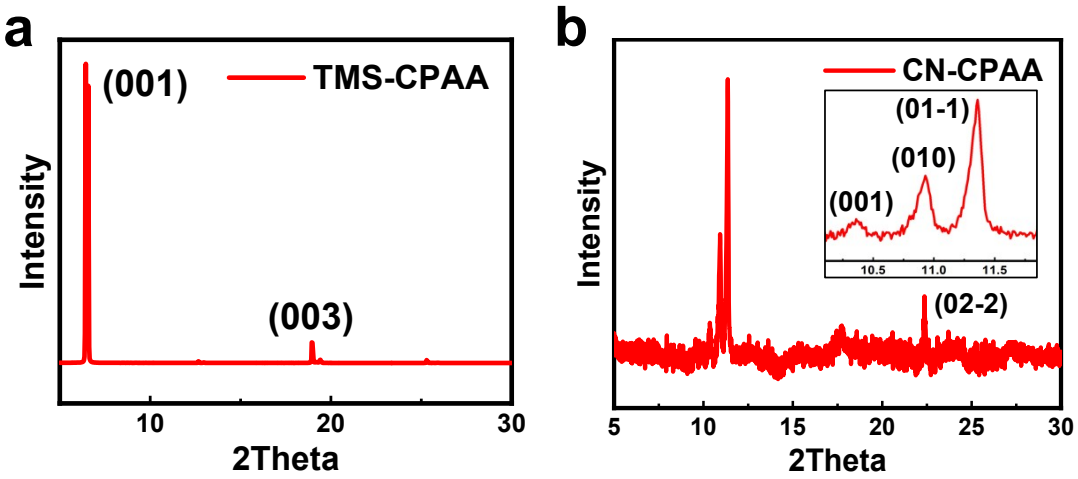

Figure S2. PXRD for TMS-CPAA and CN-CPAA

4. Calculated Electronic couplings for TMS-CPAA and CN-CPAA

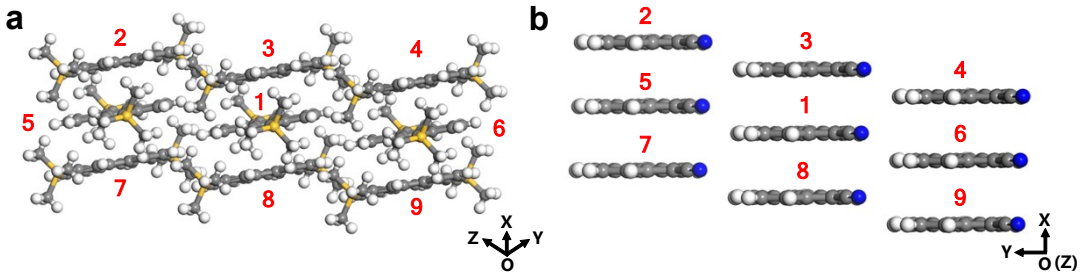

t_{13} ,t_{18}=113.6meV

t_{12}= -2.9meV ; t_{14}= -1.2meV

t_{15}= -0.5meV ; t_{16}= 0.5meV

t_{17}= -1.2meV ; t_{19}= -2.8meV

t_{13},t_{18}=-127.5meV

t_{12}= -0.2meV ; t_{14}= 5.0meV

t_{15}= 1.2meV ; t_{16}= 1.2meV

t_{17}= 5.1meV ; t_{19}= -0.2meV

Figure S3. Illustrations of molecular packing structures and transfer integrals for the nearest neighboring molecular pairs considered in the calculations for **TMS-CPAA** and **CN-CPAA**.

5. Crystallographic parameters of TMS-CPAA and CN-CPAA

Empirical formula	$C_{24}H_{26}Si_2$	$C_{20}H_8N_2$
Formula weight	370.63	276.28
Temperature/K	169.99(10)	99.9(4)
Crystal system	triclinic	triclinic
Space group	P-1	P-1
a/Å	7.2014(4)	3.7881(2)
b/Å	10.3855(6)	9.2952(8)
c/Å	15.1423(6)	9.8821(11)
α/°	108.813(5)	115.051(9)
β/°	99.184(4)	96.654(7)
γ/°	91.579(5)	92.729(6)
Volume/Å^3	1054.46(10)	311.29(5)
Z	2	1
ρ_{calc}g/cm^3	1.167	1.474
μ/mm^{-1}	1.539	0.690
Crystal size/mm^3	0.1 × 0.06 × 0.05	0.3 × 0.2 × 0.1
Radiation	CuKα (λ = 1.54184)	CuKα (λ = 1.54184)
Index ranges	-9 ≤ h ≤ 9, -12 ≤ k ≤ 13, -18 ≤ l ≤ 11	-4 ≤ h ≤ 4, -10 ≤ k ≤ 11, -11 ≤ l ≤ 12
Reflections collected	12963	1227
Independent reflections	4275 [R_{int} = 0.0871, R_{sigma} = 0.0894]	1227 [R_{int} = 0.1126, R_{sigma} = 0.0825]
Data/restraints/parameters	4275/0/241	1227/0/101
Goodness-of-fit on F^2	1.047	1.135
Final R indexes[I>=2σ(I)]	R_1 = 0.0678, wR_2 = 0.1764	R_1 = 0.0546, wR_2 = 0.1461
Final R indexes [all data]	R_1 = 0.0889, wR_2 =	R_1 = 0.0650, wR_2 =

	0.1933	0.1505

6. NMR Spectra

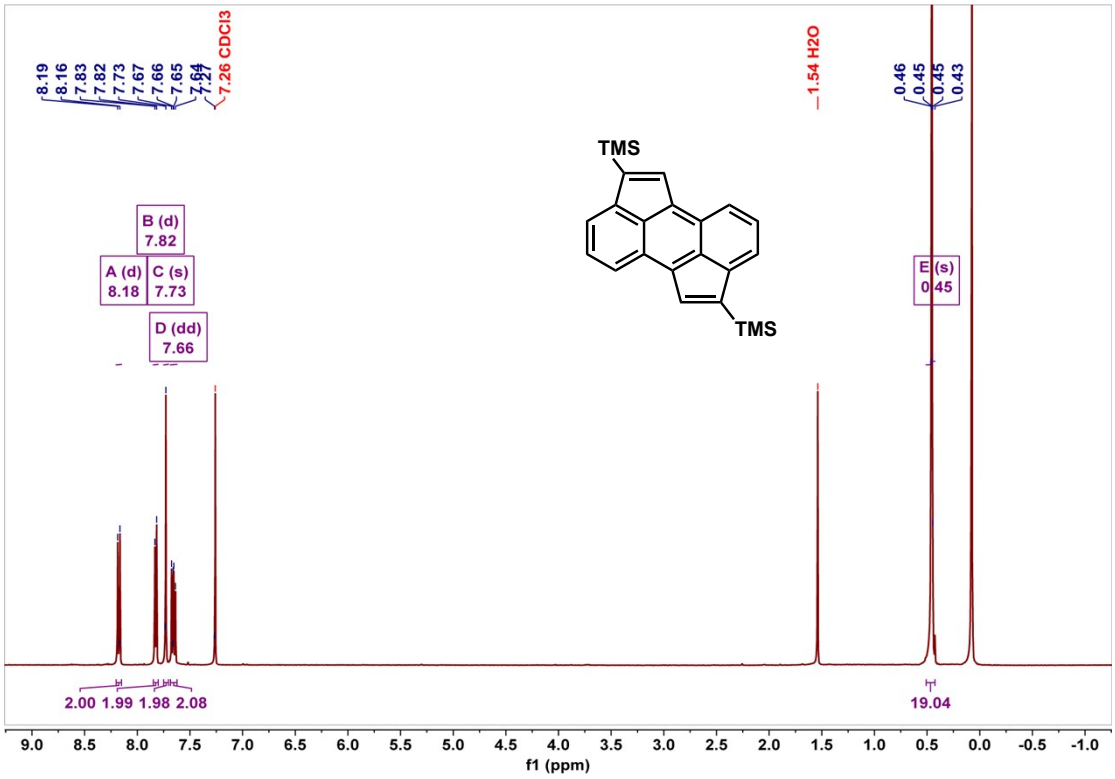

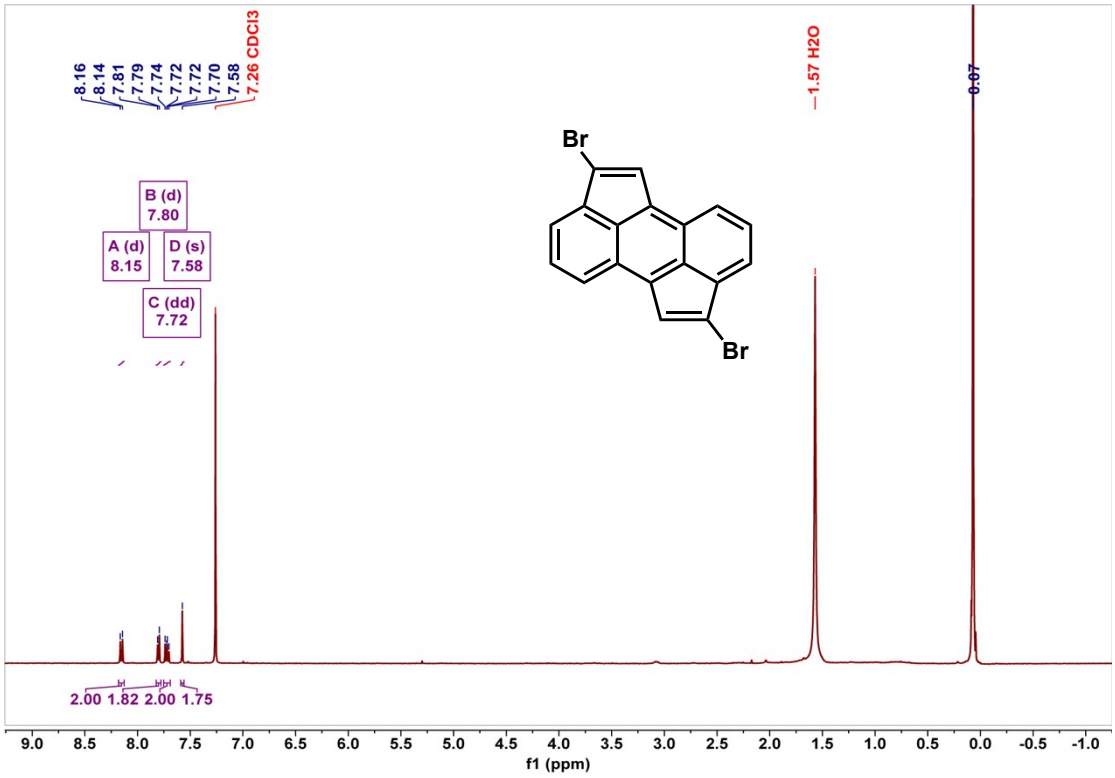

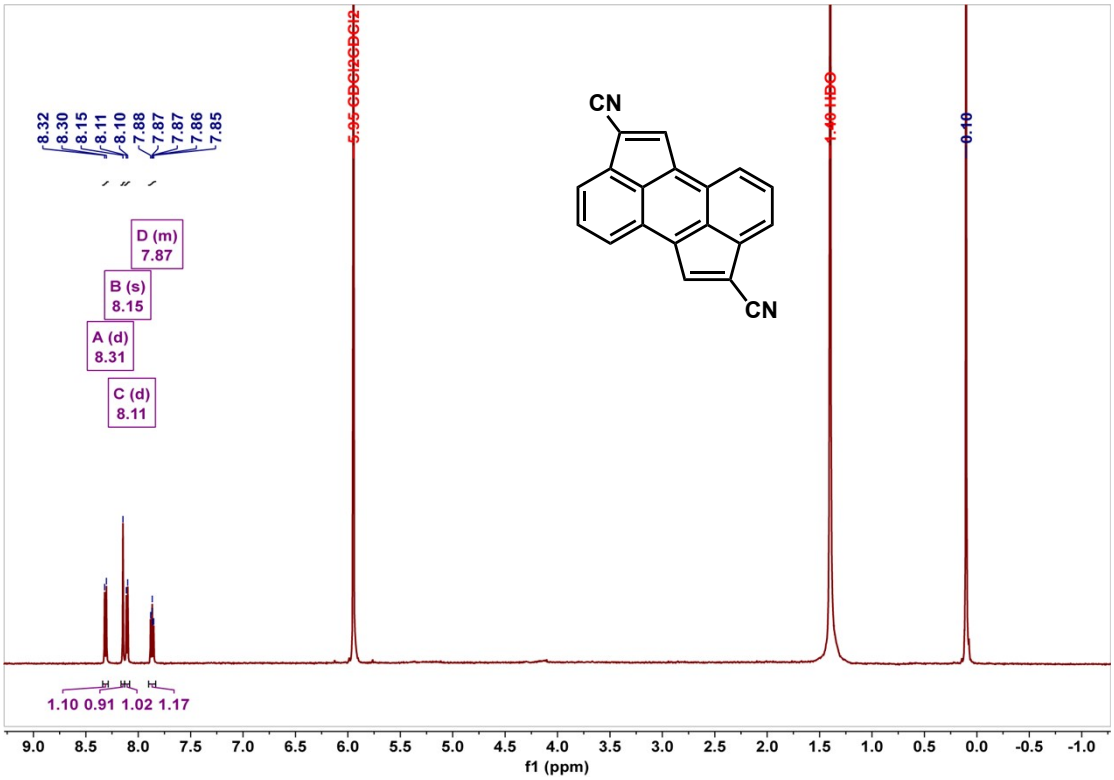
8.32
8.30
8.15
8.11
8.10
7.88
7.87
7.87
7.86
7.85
5.95
1.48
0.10
D (m)
7.87
B (s)
8.15
A (d)
8.31
C (d)
8.11
CN
CN
1.10 0.91 1.02 1.17
f1 (ppm)

7. MS Spectra

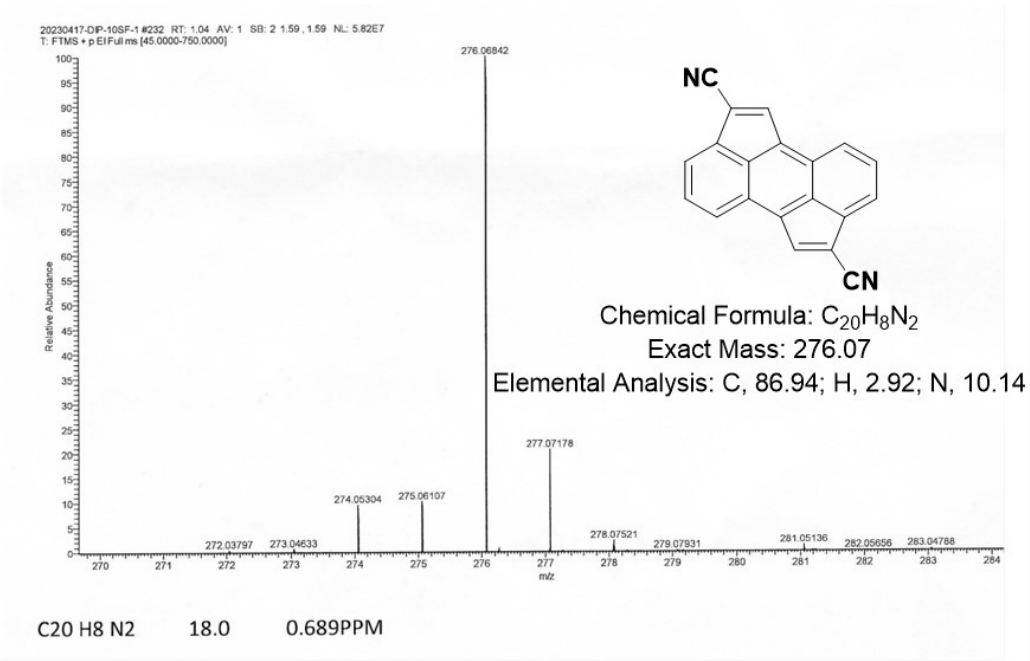
20230417-DIP-10SF-1 #232 RT: 1.04 AV: 1 SB: 2 1.59 , 1.59 NL: 5.82E7
T: FTMS + p EI Full ms [45.0000-750.0000]
276.06842
277.07178
274.05304
275.06107
272.03797
273.04633
278.07521
279.07931
281.05136
282.05656
283.04788
Relative Abundance
m/z
NC
CN
Chemical Formula: $C_{20}H_8N_2$
Exact Mass: 276.07
Elemental Analysis: C, 86.94; H, 2.92; N, 10.14
C20 H8 N2 18.0 0.689PPM

1. J. D. Wood, J. L. Jellison, A. D. Finke, L. Wang and K. N. Plunkett, *J. Am. Chem. Soc.*, 2012, **134**, 15783-15789.
2. A. D. Becke, *Phys. Rev. A*, 1988, **38**, 3098-3100.
3. Frisch, M. J.; Trucks, G. W.; Schlegel, H. B.; Scuseria, G. E.; Robb, M. A.; Cheeseman, J. R.; Scalmani, G.; Barone, V.; Mennucci, B.; Petersson, G. A.; Nakatsuji, H.; Caricato, M.; Li, X.; Hratchian, H. P.; Izmaylov, A. F.; Bloino, J.; Zheng, G.; Sonnenberg, J. L.; Hada, M.; Ehara, M.; Toyota, K.; Fukuda, R.; Hasegawa, J.; Ishida, M.; Nakajima, T.; Honda, Y.; Kitao, O.; Nakai, H.; Vreven, T.; Montgomery, Jr., J. A.; Peralta, J. E.; Ogliaro, F.; Bearpark, M.; Heyd, J. J.; Brothers, E.; Kudin, K. N.; Staroverov, V. N.; Kobayashi, R.; Normand, J.; Raghavachari, K.; Rendell, A.; Burant, J. C.; Iyengar, S. S.; Tomasi, J.; Cossi, M.; Rega, N.; Millam, N. J.; Klene, M.; Knox, J. E.; Cross, J. B.; Bakken, V.; Adamo, C.; Jaramillo, J.; Gomperts, R.; Stratmann, R. E.; Yazyev, O.; Austin, A. J.; Cammi, R.; Pomelli, C.; Ochterski, J. W.; Martin, R. L.; Morokuma, K.; Zakrzewski, V. G.; Voth, G. A.; Salvador, P.; Dannenberg, J. J.; Dapprich, S.; Daniels, A. D.; Farkas, Ö.; Foresman, J. B.; Ortiz, J. V.; Cioslowski, J.; Fox, D. J. Gaussian 09, Revision B.01,Gaussian, Inc., Wallingford CT, 2010.
4. T. Lu and F. Chen, *J. Comput. Chem.*, 2012, **33**, 580-592.
5. Z. Shuai, H. Geng, W. Xu, Y. Liao and J.-M. Andre, *Chem. Soc. Rev.*, 2014, **43**, 2662-2679.
6. L. Jiang, J. Gao, E. Wang, H. Li, Z. Wang, W. Hu and L. Jiang, *Adv. Mater.*, 2008, **20**, 2735-2740.
7. J. Laquindanum, H. Katz, A. Lovinger and A. Dodabalapur, *Chem. Mater.*, 1996, **8**, 2542-2544.
8. E. J. Meijer, C. Tanase, P. W. M. Blom, E. van Veenendaal, B. H. Huisman, D. M. de Leeuw and T. M. Klapwijk, *Appl. Phys. Lett.*, 2002, **80**, 3838-3840.
9. C. F. Macrae, I. Sovago, S. J. Cottrell, P. T. A. Galek, P. McCabe, E. Pidcock, M. Platings, G. P. Shields, J. S. Stevens, M. Towler and P. A. Wood, *J. Appl. Crystallogr.*, 2020, **53**, 226-235.